

**NANOCRYSTALS ANALYSIS OF TiO<sub>2</sub> BY X-RAY RIETVELD REFINEMENT AND TRANSMISSION ELECTRON MICROSCOPY (TEM).**Carrera, R.<sup>1,2</sup>, Castillo, N.<sup>2</sup>, Arce, E.<sup>2</sup>, Vázquez, A. L.<sup>1,2</sup>, Moran-Pineda, M.<sup>1</sup>, Montoya, J. A.<sup>1</sup>, Del Ángel, P.<sup>1</sup>, Castillo, S.<sup>1,2\*</sup><sup>1</sup>Programa de Ingeniería Molecular, Instituto Mexicano del Petróleo, D.F., México,<sup>2</sup>Departamento de Ingeniería Metalúrgica, ESIQIE-IPN, AP. 75-876, D.F. México,<sup>3</sup>CINVESTAV, Física. Av. IPN 2508,07360, D. F, México.\*correspondence author: [ascastill@imp.mx](mailto:ascastill@imp.mx)*Received: September 29th, 2008. Accepted: May 2nd, 2008**Published on-line: May 30, 2008***ABSTRACT**

Crystallographic structures of TiO<sub>2</sub> (brookite, anatase and rutile) are obtained by the Sol-Gel method. The polymorphic transition of thermodynamically unstable tetragonal anatase to stable tetragonal rutile phase is monotropic, although the degree of transformation depends on time and temperature of calcination, method of material preparation, particle size distribution, presence of impurities, etc. In this work were synthesized TiO<sub>2</sub> nanocrystals by the Sol-Gel method, these materials were annealed at 200 and 500 °C and characterized by XRD (X-ray diffraction)-Rietveld refinements, nitrogen adsorption (BET) and Transmission Electron Microscopy (TEM). Important differences were observed as a function of the annealing treatments of the samples. As for the low- temperature-treated samples (200 °C), nanocrystal with small particle sizes (7 nm) and high abundance of anatase, coexisting with the anatase and brookite phase, were obtained. Meanwhile, in the sample annealed at 500 °C, showed one particle size increased (22 nm) and an important polymorphic increased. According to the results, the sample that showed high activity in the photocatalytic decomposition of acetaldehyde was that annealed at 200 °C (TiO<sub>2</sub>-P-200).

**Keywords:** Nanostructured TiO<sub>2</sub>; polymorphic, sol-gel method; acetaldehyde decomposition.**RESUMEN**

Mediante el método sol-gel se obtuvieron las tres estructuras cristalográficas (anatasa, rutilo y broquita) del TiO<sub>2</sub>. La transición poliformica de la fase anatasa tetragonal termodinámicamente inestable a la fase estable rutilo es monotrópica, y esto depende de la temperatura y tiempo de calcinación, impurezas y del método de preparación, del cual también depende la obtención del tamaño de partícula de la TiO<sub>2</sub>. En este trabajo se sintetizó TiO<sub>2</sub> por el método sol-gel aplicando dos tratamientos térmicos a 200 y 500 °C y se les caracterizó por XRD (Difracción de rayos-X) con refinamiento Rietveld, adsorción de nitrógeno (BET) y Microscopía Electrónica de Transmisión (MET). En función de los tratamientos térmicos se observaron importantes cambios en las propiedades de las muestras sintetizadas. En la muestra tratada a baja temperatura (200 °C), se obtuvo anatasa en alta pureza con presencia de la fase broquita y el menor tamaño de partícula (7 nm). Mientras que en la muestra tratada a alta temperatura (500 °C), se incrementa su grado poliformico y el tamaño de la partícula (22 nm). De acuerdo a los resultados de la descomposición fotocatalítica del acetaldehído, la muestra activada a 200 °C (TiO<sub>2</sub>-P-200) fue la que mostró mayor actividad.

**Palabras clave:** TiO<sub>2</sub> nanoestructurada; poliformico; método sol-gel; descomposición de acetaldehído.**INTRODUCTION**

Titanium dioxide (TiO<sub>2</sub>) is the most commonly used material in electronics; ceramics, catalysis and pigment industries because of its optical and catalytic properties originate from the quantum size effect [1]. There are three types of TiO<sub>2</sub> crystalline structures: anatase, rutile, and brookite. Rutile presents the highest refractive index and is the most thermodynamically stable structure. The anatase structure is obtained at low temperatures of around 350 °C, which is useful for industrial applications

[2]. At temperatures between 400 and 800 °C, the rutile phase is also present while, at higher temperatures, only the rutile structure is present. Another possible phase present in the TiO<sub>2</sub> compounds is the brookite phase, but according some studies is present at high pressure and temperature. TiO<sub>2</sub> has become very important material due to its applications in different processes such as water purification; and more recently, the control of air contaminant gases present in indoor and outdoor environments where the UV-light is the energy source

necessary in the photocatalytic processes [3-5]. Furthermore nanometer sized particles (nanoparticles) have attracted considerable attention because of their physical and chemical characteristics. A variety of methods can be used to produce TiO<sub>2</sub> nanoparticles, including the classic sulfate process, the chloride route, the sol-gel method, the flame synthesis, and chemical vapor deposition (CVD) method. However the particle sizes and crystal structures of the resulting TiO<sub>2</sub> change with the different preparation methods considerably. The main methods [6-12] are described in Table I. According

to Table I, the described preparation methods are useful to obtain nanometric TiO<sub>2</sub>; however, through the Sol-Gel method it is possible to obtain the smallest crystal size which is a fundamental property to perform the-nearest-visible-UV photocatalytic assisted reactions; that is why TiO<sub>2</sub> is a very useful material in a variety of applications such as the decomposition of both volatile organic compounds (VOCs) and gas-phase nitrogen oxides (NO<sub>x</sub>) [13,14].

Table I. Routes to obtain TiO<sub>2</sub> nanocrystallites

MATERIALS	POWDER PROCESSING	PRECURSOR	CRYSTALLITE SIZE (nm)	COMMENTS	REF.
TiO <sub>2</sub>	Aerosol pyrolysis	Ti n-butoxide	30–80	Synthesis atmosphere and temperature affected phase transformation.	(6)
TiO <sub>2</sub> with Al and Ga	CO <sub>2</sub> láser pyrolysis	Ti isopropoxide	<100	Incorporation of Al and Ga inhibited the formation of rutile.	(7)
TiO <sub>2</sub>	Hidrothermal synthesis	Ti n-butoxide	20–65	Crystallite size and powder morphology depend on the type of	(8)
TiO <sub>2</sub>	Controlled precipitation	Ti tetra butoxide	<40	Anhydrous acetone was used as solvent and acetic acid as catalyst.	(9)
TiO <sub>2</sub>	Sol gel method	TiCl <sub>4</sub>	4–12	Ti(OH) <sub>4</sub> inorganic gel forms after reactions with ethanol and water.	(10)
TiO <sub>2</sub> and TiN	Reactive ion beam evaporation	Ti target	4–45	A high-power-density ion beam is focused on a Ti-target in a oxygen or nitrogen atmosphere (1-10 torr).	(11)
TiO <sub>2</sub>	Vapor hydrolysis	Ti tetra isopropoxide	5–65	Vapor phase precursor reacts with steam to produce a supersaturated TiO <sub>2</sub> vapor.	(12)

The Sol-Gel method allows developing the TiO<sub>2</sub> physical-chemical properties to obtain nanoparticles with both high surface area and high proportion of anatase phase; the aforementioned titania characteristics are fundamental when it is used as a catalyst in photoassisted reactions [15].

The aim of this work is the synthesis of TiO<sub>2</sub> nanocrystals by the Sol-Gel method, where these materials were annealed at 200 and 500°C and characterized by XRD-Rietveld refinements, nitrogen adsorption (BET) and Transmission Electron Microscopy (TEM) of Polymorphic Titanium dioxide (TiO<sub>2</sub>), for its application

as a catalyst in the acetaldehyde photodecomposition through *in situ* photoassisted micro reactions (in a cell) assisted with UV light.

## EXPERIMENTAL

TiO<sub>2</sub> nanocrystal were obtained by sol gel method using as organometallic (OM) precursor titanium isopropoxide, [Ti{OCH(CH<sub>3</sub>)<sub>2</sub>}<sub>4</sub>], which is liquid at room temperature (melting point 20 °C), and 2-propanol as solvent, under reflux at 70°C and uniform stirring at pH 2 to obtain 10 g of TiO<sub>2</sub>. Afterwards, the obtained product was dried at 70 °C during 12 h; and then, it was ground. Finally the

products were calcined during 3 h at 200°C; and the other one at 500°C. The samples were labeled as TiO<sub>2</sub> - P200 and TiO<sub>2</sub>- P500.

In order to perform the XRD, a D500 Siemens with a copper tube and K $\alpha$  radiation of 1.5405; operating at 35 KeV and 15mA was used. The intensities were determined in the 2 $\theta$  interval ranging from 20° to 80°. To refine each spectrum, the Rietveld analysis was applied by using the Full Prof software by Rodríguez Carvajal [16,17] (Figure 1). The crystal size was determined by the Scherrer equation [18,19].

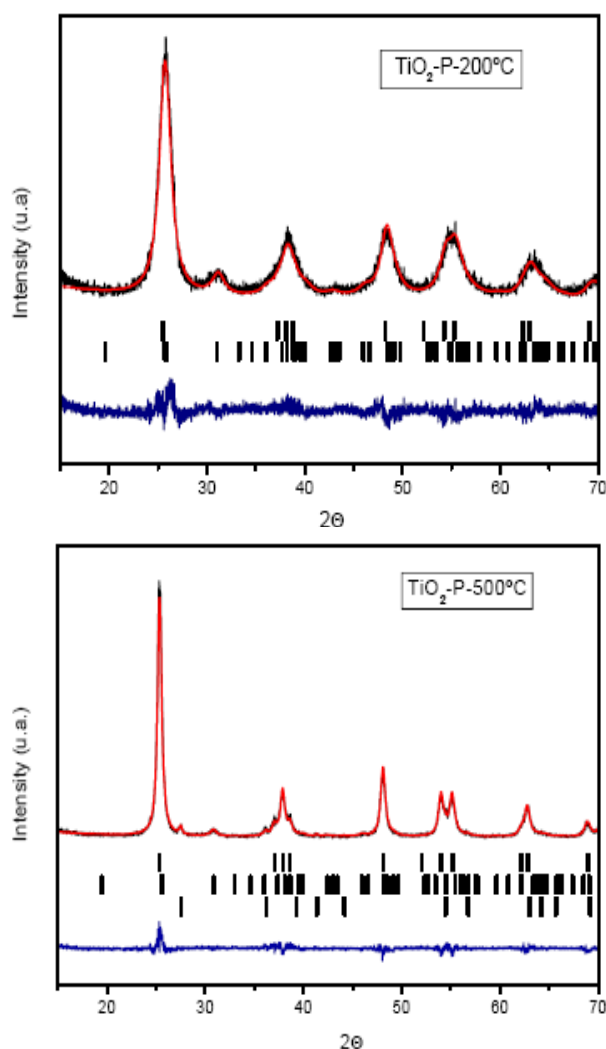


Fig.1. Rietveld refinement plots of sol-gel catalysts. TiO<sub>2</sub>-P-200 °C, the upper tick marks correspond to anatase and the lower thick marks correspond to brookite. TiO<sub>2</sub>-P-500 °C, the upper thick marks correspond to anatase, the middle tick marks

The determination of the surface area, pore volume and pore size distribution of the TiO<sub>2</sub> calcined at 200 y 500°C was performed by means of the nitrogen physisorption in an ASAP-2000 Micrometrics equipment. The specific area was determined by the BET method through the nitrogen adsorption isotherms at -196°C. Both, the volume and pore size distribution were calculated from the BET isotherms by the BJH method (Barret, Joyner, Halenda) (Figure 2).

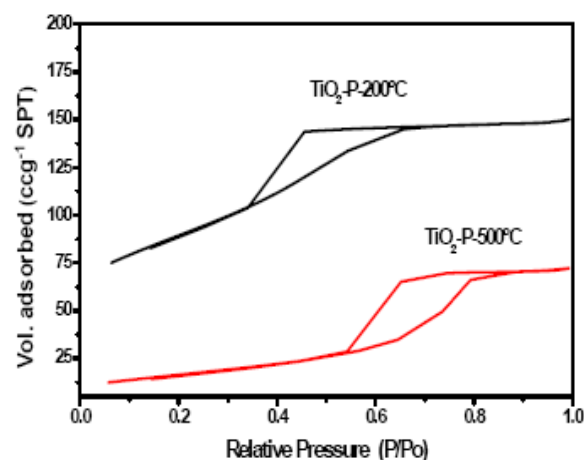


Fig. 2. Profiles of N<sub>2</sub> isotherms Adsorption-desorption: TiO<sub>2</sub>-P200 and TiO<sub>2</sub>-P500

The determination of the TiO<sub>2</sub> crystal size was performed by the Transmission Electron Microscopy (TEM) by means of a Transmission Electron Microscope Jeol 100 (X) with a resolution ranging from 2 to 5Å working at 100 kV. From the obtained micrographs, the average particle size was calculated by the surface/volume equation [20].

The photocatalytic activity tests for the TiO<sub>2</sub>-P-200, TiO<sub>2</sub>-P-500 and the witness (Degussa P25) were carried out in automated experimental equipment at microreaction level. A quartz cell was used as photoreactor with a 365-UV lamp (UVP-Light-Sources) with a 100 μW/cm<sup>2</sup> intensity.

The tests were carried out at ambient conditions with an acetaldehyde (CH<sub>3</sub>CHO) concentration of 300 ppmv and 2% of oxygen by means of a 365-nm UV lamp. The

photocatalytic activity was determined by the acetaldehyde ( $\text{CH}_3\text{CHO}$ ) determined by the  $\text{CH}_3\text{CHO}$  concentration change and the  $\text{CO}_2$  formation.

## RESULT AND DISCUSSION

The effect of the calcination temperature on the surface area in the samples is very important for instance in the sample activated at 200 °C ( $\text{TiO}_2\text{-P-200}$ ), this value is tripled ( $189 \text{ m}^2/\text{g}$ ) with respect to that ( $60 \text{ m}^2/\text{g}$ ) in the activated sample at 500°C ( $\text{TiO}_2\text{-P500}$ ). According to the BET results, the sample  $\text{TiO}_2\text{-P-200}$  showed high pore volume ( $0.17 \text{ cc/g}$ ) and less mean pore diameter ( $36 \text{ \AA}$ ), compared with were calcined at 500 °C, which results were  $0.11 \text{ cc/g}$  and  $74 \text{ \AA}$ , respectively (Figure 2). Both catalysts showed characteristics of the hysteresis loops typical of the mesopore structures in type IV [21].

Likewise, there was also a thermal effect on the  $\text{TiO}_2$  crystal size which was determined by TEM; where there was a 2.4-time crystal size increment as a consequence of the sinterization process (Table III) [22]. By the XRD

and Rietveld refinement, the phases and structures formed in each of the  $\text{TiO}_2$  samples were determined using the unit cells and space groups known (Table II). Figure 2 shows typical refinements plots obtained by using these unit cells and corresponding to samples  $\text{TiO}_2\text{-P200}$  and  $\text{TiO}_2\text{-P500}$ . In the sample annealing at 200 °C was less polymorphic (anatase-brookite phases) than the annealing at 500 °C (anatase-brookite-rutile phases).

Table II. Space groups and atomic fractional coordinates of titania phases

<b>Anatase: space group I4/amd</b>				
Atom	Site	x	y	z
Ti	4a	0.0	0.75	0.125
O	8e	0.0	0.25	<i>u</i>
<b>Brookite: space group Pbcu</b>				
Ti	8c	0.127	0.113	-0.127
O(1)	8c	0.010	0.155	0.180
O(2)	8c	0.230	0.105	0.465
<b>Rutile: space group P4<sub>2</sub>/mnm</b>				
Ti	4a	0.0	0.0	0.0
O	8e	<i>v</i>	<i>v</i>	0.0

Note: values of *u* and *v* according Table3.

Table III. XRD-Rietveld refinement phase concentration and crystal size of sol-gel  $\text{TiO}_2$  samples

SAMPLES	STRUCTURE	% PHASES	CRYSTAL SIZE (nm)	CRYSTAL SIZE SCHERRER (nm)	PHASE	a (nm)	b (nm)	c (nm)
$\text{TiO}_2\text{-P-200}$	Tetragonal	62.88	6.96	7.03	Anatase	0.3790926	0.3790926	0.9495732
	Orthorhombic	37.12	6.09	18.26	Brookite	0.9167624	0.5416461	0.5210546
$\text{TiO}_2\text{-P-500}$	Tetragonal	82.67	20.5	22.04	Anatase	0.3786167	0.3786167	0.9506104
	Orthorhombic	14.9	13.1	34.02	Brookite	0.9142567	0.5442068	0.5191934
	Monoclinic	2.43	34.72	27.14	Rutile	0.4591337	0.4591337	0.2951845

In Figure 3, it is possible to see that anatase tetragonal structure is the predominant phase in both samples; nevertheless, it is found in a higher proportion in the  $\text{TiO}_2\text{-P500}$  sample; in addition, in this sample, it is also found the monoclinic structure (rutile). As for the orthorhombic structure (brookite), the highest proportion is found in the  $\text{TiO}_2\text{-P200}$  sample; in this sample, anatase and brookite without rutile are found with small crystallite size ( $\approx 6 \text{ nm}$ ), which could give specific photocatalytic properties to that sample because of the

nanometric crystal size/phase composition ratio [23]. By the Rietveld refinement, the  $\text{TiO}_2\text{-P200}$  and  $\text{TiO}_2\text{-P500}$  samples showed the phases compositions described in Table III. According to these results, we can see that the handling of the variables concerning the Sol-Gel method enabled us to obtain anatase at low temperature (200°C) since the anatase phase transformation by other methods occurs from 450°C [24]. It is suggested that the small crystallite size control the anatase-rutile transition and its stability likewise, the method used allows us to obtain

brookite at low temperature [25]. Likewise, it is known that the brookite-rutile transformation is faster than anatase-rutile transformation, where, there is an effect related with the pressure on small anatase crystallites, in which case could promote the formation of a rutile nucleus in a

short transition temperatures, but in this work even at high temperature the anatase-rutile transition does not occur, therefore, it could be probably that the anatase-rutile transition may be modified, when the grain size was enough small [26,27].

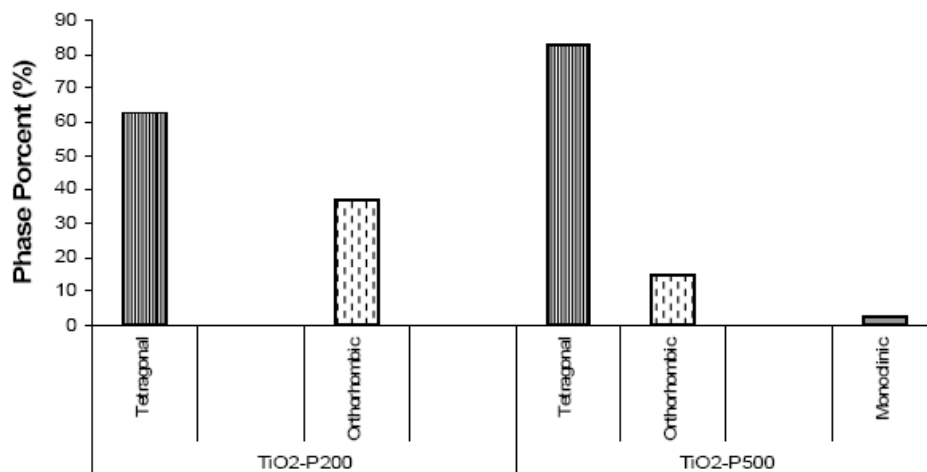


Fig. 3 XRD-Rietveld refinement concentrations for each structure in the sol-gel TiO<sub>2</sub>

Structure of the polycrystals and their interplanar distances in the TiO<sub>2</sub>-P-200 and TiO<sub>2</sub>-P-500 samples corresponding to the TiO<sub>2</sub> tetragonal phase (anatase) was determined by TEM. In Figure 4 it can be seen that the average nanometric size of the crystals of TiO<sub>2</sub>-P-200 is around 7nm; and their corresponding diffraction pattern. By selecting one crystal, the individual diffraction pattern was obtained which presents a tetragonal structure in the B (111) direction which corresponds to the anatase phase with an interplanar distance of 0.323 nm. In Figure 5 nanocrystal of TiO<sub>2</sub> P200 with morphology characteristic of tetragonal structure can be observed. By this technique it was also determined the average distribution of the crystal size as it is shown in Figure 6 with an average size of 7 nm and a standard distribution of 1.32 nm which confirms the presence of nanostructured TiO<sub>2</sub>.

While for TiO<sub>2</sub>-P-500 in Figure 7A it can be observed that the average nanometric size of the crystals is of 17nm; and in the Figure 6B their corresponding diffraction pattern.

By selecting one crystal, the individual diffraction pattern was obtained which presents a tetragonal structure in the (112) direction which corresponds to the anatase phase with an interplanar distance of 0.323 nm, Figure 7B.

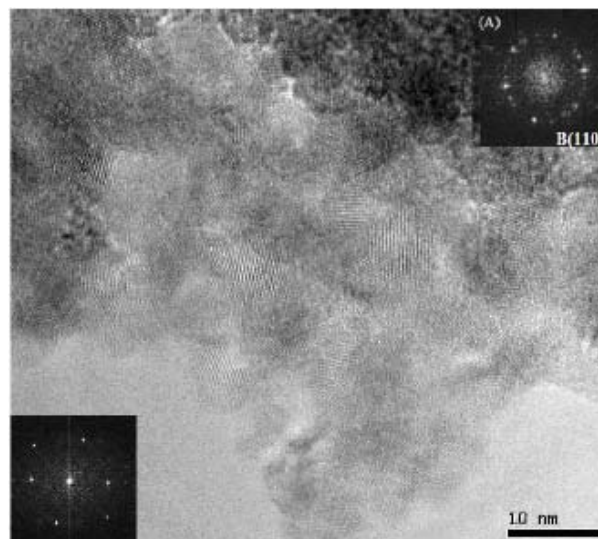
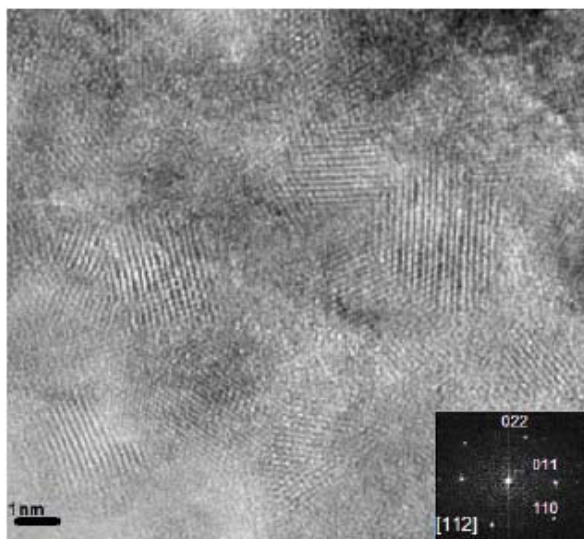
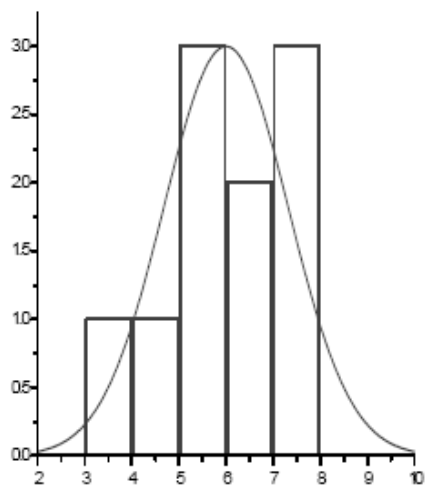


Fig. 4. Polymorphic nanocrystals of TiO<sub>2</sub>-P-200. A) diffraction pattern of the TiO<sub>2</sub>.

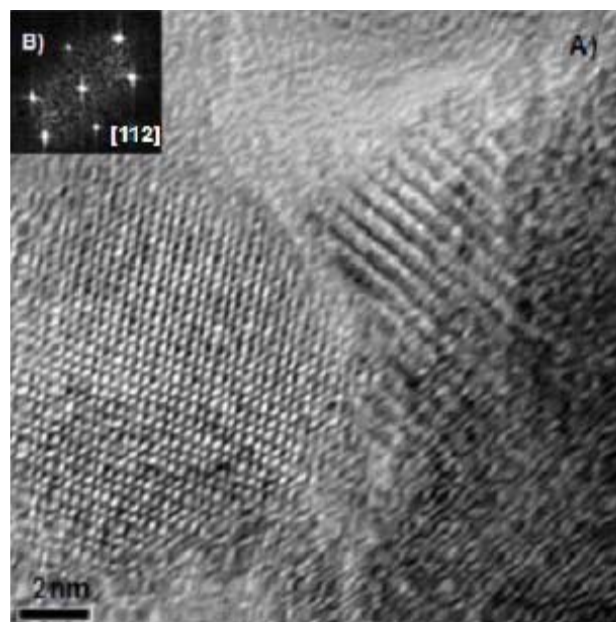
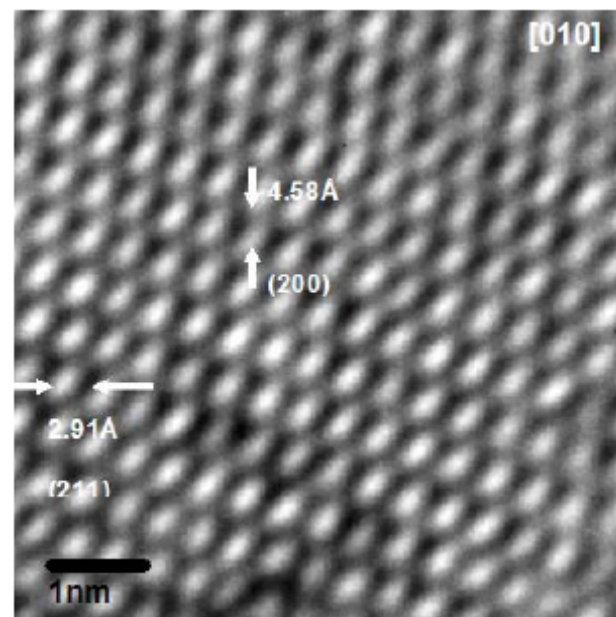
Fig. 5. Details of TiO<sub>2</sub>-P-200 nanocrystal.Fig. 6 Average crystal size (SD = 1.32 nm) of sol-gel TiO<sub>2</sub> samples.

Likewise, in Figure 8 is showed a single crystal of TiO<sub>2</sub>-P-500 with the morphology characteristic in tetragonal structure. The morphology of the TiO<sub>2</sub> nanostructured materials is equiaxial.

The photocatalytic activity in the TiO<sub>2</sub>-P200, TiO<sub>2</sub>-P500 and the witness (TiO<sub>2</sub>- Degussa P25) samples was evaluated by measuring the acetaldehyde (CH<sub>3</sub>CHO) concentration change and the CO<sub>2</sub> formation as a function of the UV radiation time.

According to the obtained results, the catalyst that presented the highest activity in the acetaldehyde photodecomposition and the best selectivity towards the

CO<sub>2</sub> formation was the TiO<sub>2</sub>-P200 which yielded a CH<sub>3</sub>CHO concentration of 12.5 ppmv and a CO<sub>2</sub> selectivity of 149 ppmv by the end of the stated evaluation time (150 min); whereas in the witness sample (TiO<sub>2</sub>-Degussa P25), the concentration and selectivity were of 200 ppmv and 33 ppmv, respectively, Figures 9 and 10.

Fig. 7. A) Nanocrystals of TiO<sub>2</sub>-P-500 B) Diffraction pattern of the TiO<sub>2</sub>.Fig. 8. Details of nanocrystal of TiO<sub>2</sub>-P-500

It could be observed that in the induction period of around 30 min is detected less CO<sub>2</sub> formation, where this period is attributed to initial oxidation of acetaldehyde giving absorbed acetic acid, which after saturation of the surface is decomposed and total mineralization is reached [28]. The photocatalytic activity and selectivity of the Sol-Gel TiO<sub>2</sub> catalysts are 1.5 and 4 times higher, respectively, than those shown by the commercial catalyst (TiO<sub>2</sub>- Degussa P-25).

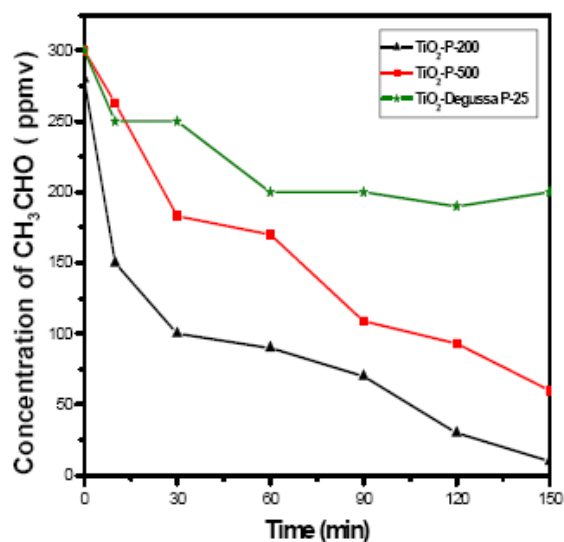


Figure 9 Acetaldehyde conversions a function of time for the TiO<sub>2</sub> samples

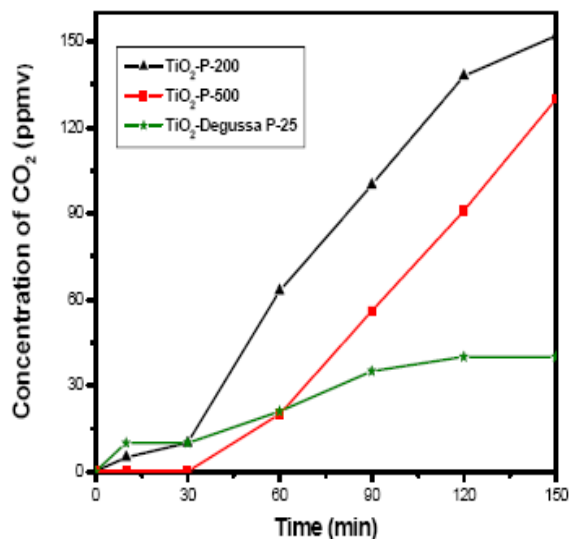


Fig. 10. CO<sub>2</sub> selectivity in acetaldehyde decomposition in TiO<sub>2</sub> samples

## CONCLUSIONS

By varying the Sol-Gel parameters, it was possible to obtain less polymorphic TiO<sub>2</sub> at low temperature, since the TiO<sub>2</sub>-P200 showed only two phases (anatase and brookite); and a small crystal size ( $\approx 7$  nm), whereas the TiO<sub>2</sub>-P500 sample showed the three main structures (tetragonal, orthorhombic and monoclinic); likewise, a bigger crystal size ( $> 22$  nm). In the same way, handle the sol-gel method parameters it was possible to increase the surface area (189 m<sup>2</sup>/g). The TiO<sub>2</sub> with less polymorphism and small crystal size showed high photoactivity in the acetaldehyde decomposition; therefore, these two variables could play a major role in photocatalysis, mainly in the decomposition of VOCs in both indoor and outdoor environments.

## ACKNOWLEDGEMENTS

We acknowledge the support given to us by the Molecular Engineering Program (IMP) and CINVESTAV (IPN). The authors thank Technician Rufino Velázquez for his assistance and technical support in this work.

## REFERENCES

- [1] Kim, C. S., Okuyama K., Nakaso K, and Shimada, M. (2004) "Direct Measurement of Nucleation and Growth Modes in Titania Nanoparticles Generation by a CVD Method" *J Chem Eng Jpn* 37: 1379-1389.
- [2] Mergel, D.; Buschendorf, D.; Eggert, S.; Grammes R.; Samset, B. (2000) "Density and refractive index of TiO<sub>2</sub> films prepared by reactive evaporation" *Thin Solid Films* 371: 218-224.
- [3] Fujishima A., Zhang C.R. (2000) "Titanium dioxide photocatalysis: present situation and future approaches" *Chimie* 9: 750-760.
- [4] Anpo M. "Utilization of TiO<sub>2</sub> photocatalysts in green chemistry" (2000) *Pure Appl Chem* 72: 1265-1270.

- [5] Hashimoto K., Irie H., Fujishima A. (2005) "TiO<sub>2</sub> Photocatalysis: A Historical Overview and Future Prospects" *Jap J Appl Phys* 44: 8269-8285.
- [6] Ahonen P.P., Kauppinen E.I., Journet J.C., Deschavernes J.L., Van Tendeloo G.J. (1999) "Preparation of nanocrystalline titania powder via aerosol pyrolysis of titanium tetrabutoxide" *Mater Res* 14: 3938-3948.
- [7] Depero L.E., Marino A., Allieri B., Bontempi E., Sangaletti L., Casale C., Notaro M. (2000) "Morphology and microstructural properties of TiO<sub>2</sub> nanopowders doped with trivalent Al and Ga cations" *J Mater Res*: 2080-2086.
- [8] Yang J., Mei S., Ferreira J.M.F. (2001) "Hydrothermal synthesis of nanosized titania powders: influence of tetraalkyl ammonium hydroxides on particle characteristics" *J Amer Ceram Soc* 84:1696-1702.
- [9] Mayadevi S., Kulkarni S.S., Patil A.J., Shinde M.H., Potdar H.S., Deshpande S.B., Date S. K. (2000) "Chemically precipitated titania for membrane applications – effect of heat treatment and fabrication conditions on its performance" *J Mater Sci* 35: 3943–3949.
- [10] Zhu Y. H., Zhang L., Gao C., Cao L. (2000) "The synthesis of nanosized TiO<sub>2</sub> powder using a sol-gel method with TiCl<sub>4</sub> as a precursor" *J Mat Sci* 35: 4049-4054.
- [11] Nakagawa Y., Grigoriu C., Masugata K., Jiang W., Yatsui K. (1998) "Synthesis of TiO<sub>2</sub> and TiN nanosize powders by intense light ion-beam evaporation" *J Mater Sci* 33: 529-533.
- [12] Zhang Y. H., Chan C.K., Porter J.F., Guo W. (1998) "Micro-Raman spectroscopic characterization of nano-sized TiO<sub>2</sub> powders prepared by vapor hydrolysis" *J Mater Res* 13: 2602-2609.
- [13] Cao L., Gao Z., Suib S.L., Obee T.N., Steven O.H., Freihaut J.D. (2000) "Photocatalytic Oxidation of Toluene on Nanoscale TiO<sub>2</sub> Catalysts: Studies of Deactivation and Regeneration" *J Catal* 196: 253-261.
- [14] Benoit-Marquie F., Wilkenhoner U., Simon V., Braun A., Oliveros E., Maurette M.T. (2000) "VOC photodegradation at the gas-solid interface of a TiO<sub>2</sub> photocatalyst - Part I: 1-butanol and 1-butylamine" *J Photochem and Photobiol A: Chem* 132: 225-232.
- [15] Castillo S., Gómez R., Morán-Pineda M. (2003) "Effect of sol-gel derived Al<sub>2</sub>O<sub>3</sub>-ZrO<sub>2</sub> and Al<sub>2</sub>O<sub>3</sub>-TiO<sub>2</sub> oxides on the selectivity of NO reduction by CO under oxidizing conditions" *React Kinet Lett* 79: 217-279.
- [16] Rodríguez-Carbajal J. (1993) "Determination of the crystallized fractions of a largely amorphous multiphase material by the Rietveld method" *J Phys B* 192: 55-69.
- [17] Orlhac X., Fillet C., Deniard P., Dulac A.M., Brec R. (2001) "Determination of the crystallized fractions of a largely amorphous multiphase material by the Rietveld method" *Appl Cryst* 34: 114-118.
- [18] Fuentes L. (1998) *Análisis de minerales y el método de Rietveld*, México, Sociedad Mexicana de Cristalografía, pp.78.
- [19] Reid J.W., Hendry J.A. (2006) "Rapid, accurate phase quantification of multiphase calcium phosphate materials using Rietveld refinement" *Appl Cryst* 39: 536-543.
- [20] Castillo S., Morán-Pineda M., Molina V., Gómez R., López T. (1998) "Catalytic reduction of nitric oxide on Pt and Rh catalysts supported on alumina and titania synthesized by the sol-gel method" *Appl Catal B: Environ* 15: 203-209.
- [21] J.A. Wang, A. Cuan, J. Salmenes, N. Nava, S.Castillo, M. Morán-Pineda, F. Rojas, (2004), "Studies of sol-gel TiO<sub>2</sub> and Pt/TiO<sub>2</sub> catalysts for NO reduction by Co in a oxygen-rich condition", *Appl. Surf. Sci.* 230, 94-105.

- [22] Song, S.H., Wang X., Xiao P., (2002) “Synthesis of nanosized rutile TiO<sub>2</sub> powder at low temperature” *Mater Chem Phys* 77: 314-317.
- [23] Wang J.A., Lima-Ballesteros R., López T., Moreno A., Gómez R, Novaro O., Bokhimi X., (2001) “Quantitative determination of titanium lattice defects and solid.state reaction mechanism in iron-doped TiO<sub>2</sub> photocatalysts” *J Phys Chem B* 105: 9692-9698..
- [24] Ovenstone J. (2001) “Preparation of novel titania photocatalysts with high activity” *J Mater Sci* 36: 1325-1329.
- [25] Radhica C. Bhave, Burtrand I. Lee, (2007) “Experimental variables in the synthesis of brookite phase TiO<sub>2</sub> nanoparticles”, *Materials Science and Engineering A*, 467, 146-149.
- [26] A.A. Gribb, J.F. Banfield, (1997) “Particle size effects on transformation kinetics and phases stability in nanocrystalline TiO<sub>2</sub>”, *Am. Mineral*, 82, 717-728.
- [27] Ke-Rong Zhu, Ming-Sheng Zhang, Jian-Ming Hong, Zhen Yin, (2005) “Size effect on phase transition sequence of TiO<sub>2</sub> nanocrystal”, *Matter. Sci. Eng. A*, 403, 87-93.
- [28] Ulrike Diebold, (2003) “The surface science of titanium dioxide”, *Surf. Sci. Reports*, 48, 53-229.